Journal of Medicinal Chemistry

ARTICLE

pubs.acs.org/jmc

Synthesis and Biological Evaluation of Novel 5-Benzylidenethiazolidine-2,4-dione Derivatives for the Treatment of Inflammatory Diseases

Liang Ma,[†,§] Caifeng Xie,[†,§] Yinghua Ma,[†,§] Juan Liu,[†] Mingli Xiang,[*,†] Xia Ye,[†] Hao Zheng,[†] Zhizhi Chen,[†] Qinyuan Xu,[†] Tao Chen,[†] Jinying Chen,[†] Jincheng Yang,[†] Neng Qiu,[†] Guangcheng Wang,[†] Xiaolin Liang,[†] Aihua Peng,[†] Shengyong Yang,[†] Yuquan Wei,[†] and Lijuan Chen[*,†]

[†]State Key Laboratory of Biotherapy, West China Hospital, West China Medical School, Sichuan University, Keyuan Road 4, Gaopeng Street, Chengdu 610041, China

Supporting Information

ABSTRACT: Twenty-two compounds based on thiazolidine-2,4-dione moiety were synthesized and evaluated for the inhibitory potency on the production of nitric oxide (NO), inducible nitric oxide synthase (iNOS) activity, and the generation of prostaglandin E_2 (PEG_2). (*Z*)-*N*-(3-Chlorophenyl)-2-(4-((2,4-dioxothiazolidin-5-ylidene) methyl) phenoxy) acetamide (**3I**), superior to the commercial anti-inflammatory drug indomethacin, significantly inhibited iNOS activity (IC_{50} = 8.66 μM), iNOS-mediated NO, and cyclooxygenase (COX)-2-derived PGE_2 production (IC_{50} = 4.16 and 23.55 μM, respectively) on lipopolysaccharide (LPS)-induced RAW 264.7 cells. Docking study revealed that **3I** was perfectly docking into the active site of murine iNOS and suppressed the expression of iNOS protein as evidenced by Western blot analysis. At the dose of 50 mg/kg, oral administration of **3I** possessed protective properties in both carrageenan-induced paw edema and adjuvant-induced arthritis rat models.

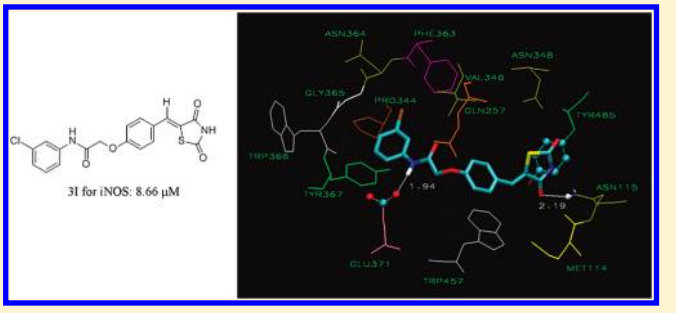

INTRODUCTION

Inflammation is a complex process involving numerous mediators of cellular and plasma origin with interrelated biological effects. Macrophages, neutrophils, and lymphocytes are important that have been implicated in the pathogenesis of acute and chronic inflammatory diseases.[1,2]

Proinflammatory stimulus activate cellular responses and regulate inflammatory and immune functions including the recruitment of macrophages and production of proinflammatory cytokines.[3] Macrophages produce nitric oxide (NO) and up-regulate prostaglandins (PGs), interleukin-1β (IL-1β), and tumor necrosis factor-α (TNF-α) in the inflammatory process. NO, being an endogenous free radical, is an important and unique mediator in the process of vasodilation, nonspecific host defense, and acute or chronic inflammation.[4−6] NO is generated via the oxidation of L-arginine to L-citrulline by nitric oxide synthase (NOS) isoforms in an nicotinamide adenine dinucleotide phosphate (NADPH)- and O_2-dependent process.[7] There are at least three isoforms of the NOS enzyme: endothelial (eNOS), neuronal (nNOS), and inducible (iNOS). Because iNOS is responsible for the overproduction of NO in inflammation, it has become a new target for drug development in the treatment of inflammatory diseases. Normally, NO is sustained at a low level when stimulated by various inflammatory stimulus (e.g., proinflammatory cytokines or lipopolysaccharide (LPS)), iNOS produces a high level of NO and induces tissue injury at the inflammatory site.[8] Considerable evidence have shown that overproduction of NO induced by iNOS has been implicated in various pathological diseases including septic shock, tissue damage, and rheumatoid arthritis (RA).[9] Prostaglandin E_2 (PGE_2), one product of the PGs, is a proinflammatory mediator and derived by the cyclooxygenase-1/2 (COX-1/2) pathway.[10] PGE_2 regulates vascular permeability, platelet aggregation, and thrombus formation in the development of inflammation. Inhibition of PGE_2 production reduces the deleterious consequences of inflammatory diseases.[11] Therefore, suppression of overproduction of NO and PGE_2 might be useful for the treatment of inflammatory diseases.

Thiazolidinediones (TZDs), ligands for peroxisome proliferator-activated receptor-γ (PPAR-γ), exert anti-inflammatory effects independent of the insulin sensitizing effect.[12] Natural and synthetic ligands of PPAR-γ have been shown to inhibit the production of several inflammatory cytokines including IL-1β and TNF-α by macrophages in vitro and blockade inflammatory developments.[13,14] In vivo study has revealed that PPAR-γ is a modulator of inflammation including the down-regulation of level of iNOS and NO.[15,16] PPAR-γ agonists reduce iNOS

Received: September 7, 2010
Published: March 07, 2011

Scheme 1. General Synthesis of 3Q−V[a]

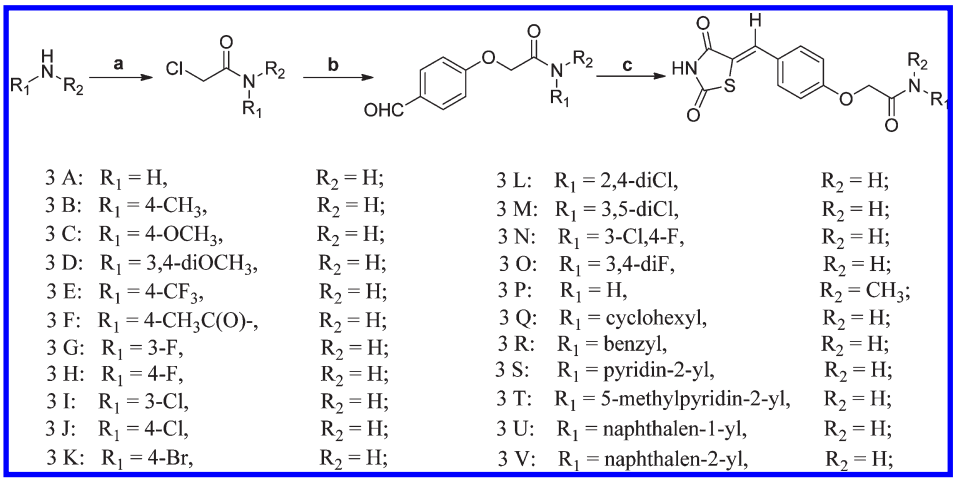

3 A:	R_1 = H,	R_2 = H;	
3 B:	R_1 = 4-CH_3,	R_2 = H;	
3 C:	R_1 = 4-OCH_3,	R_2 = H;	
3 D:	R_1 = 3,4-diOCH_3,	R_2 = H;	
3 E:	R_1 = 4-CF_3,	R_2 = H;	
3 F:	R_1 = 4-$CH_3C(O)$-,	R_2 = H;	
3 G:	R_1 = 3-F,	R_2 = H;	
3 H:	R_1 = 4-F,	R_2 = H;	
3 I:	R_1 = 3-Cl,	R_2 = H;	
3 J:	R_1 = 4-Cl,	R_2 = H;	
3 K:	R_1 = 4-Br,	R_2 = H;	
3 L:	R_1 = 2,4-diCl,	R_2 = H;	
3 M:	R_1 = 3,5-diCl,	R_2 = H;	
3 N:	R_1 = 3-Cl,4-F,	R_2 = H;	
3 O:	R_1 = 3,4-diF,	R_2 = H;	
3 P:	R_1 = H,	R_2 = CH_3;	
3 Q:	R_1 = cyclohexyl,	R_2 = H;	
3 R:	R_1 = benzyl,	R_2 = H;	
3 S:	R_1 = pyridin-2-yl,	R_2 = H;	
3 T:	R_1 = 5-methylpyridin-2-yl,	R_2 = H;	
3 U:	R_1 = naphthalen-1-yl,	R_2 = H;	
3 V:	R_1 = naphthalen-2-yl,	R_2 = H;	

[a] Reagents and conditions: (a) 2-chloroacetyl chloride, Et_3N, CH_2Cl_2, 0−25 °C, 20 h; (b) KI, K_2CO_3, 4-hydroxybenzaldehyde, reflux, 24 h; (c) thiazolidine-2,4-dione, β-alanine, AcOH, reflux, 4 h.

expression and NO production in macrophages, mesangial cells, and other inflammatory cells.[17] A novel small-molecule inhibitor AS605240,[18] one of TZD derivatives, effectively suppressed the progression of joint inflammation and damage in both lymphocyte-independent and lymphocyte-dependent mouse models of RA. These results encourage us to develop novel agents for the treatment of NO and iNOS related inflammatory diseases.

In the present study, 22 compounds based on thiazolidine-2,4-dione moiety were synthesized and evaluated for the biological studies. Subsequently, (*Z*)-*N*-(3-chlorophenyl)-2-(4-((2,4-dioxothiazolidin-5-ylidene) methyl)phenoxy)acetamide (**3I**) was identified as the most potent chemical molecule. The IC_{50} values of **3I** on iNOS activity, the production of iNOS-mediated NO and COX-2-derived PGE_2 were 8.66, 23.55, and 4.16 μM, respectively, on LPS-induced RAW 264.7 cells. Western blot analysis further revealed that **3I** inhibited LPS-induced iNOS and COX-2 protein expressions in a dose-dependent manner. Furthermore, two inflammatory models from carrageenan-induced paw edema in ICR mice and an adjuvant-induced arthritis in rats demonstrated that **3I** exhibited significantly anti-inflammatory activity.

CHEMISTRY

Various amines in this study were converted into chloroacetamide derivatives with excellent yields via a reaction employed 2-chloroacetyl chloride in the presence of triethylamine as base and using dichloromethane as solvent. The pivotal aldehyde intermediates were synthesized through the use of chloroacetamide derivatives, 4-hydroxybenzaldehyde, potassium carbonate as base, and potassium iodide as catalyst according to Scheme 1, and then, to obtain the 22 targeted compounds varying with the western substituted group quickly, the Knoevenagel reaction which accomplished by condensation aldehyde intermediate with thiazolidine-2,4-dione was performed in parallel using EYELA Personal Organic Synthesizer (Tokyo, Rikakikai) with a 12-well liquid-phase reaction block.

In theory, *E* and *Z* geometrical isomers around the exocyclic double bond (CH═C) are possible for 5-benzylidenethiazolidine-2,4-dione derivatives. However, on the basis of literature data for similar compounds, the *Z*-configuration has been reported thermodynamically more stable than the *E*-configuration.[19,20]

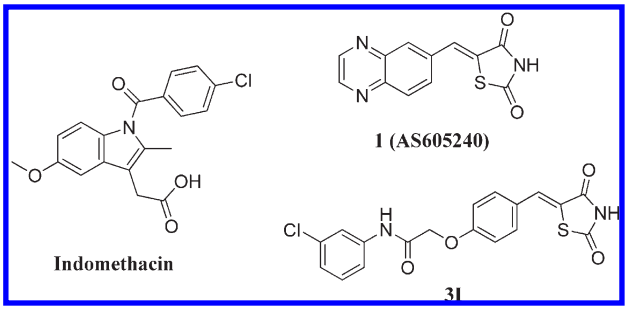

Figure 1. Chemical structure of indomethacin, **1**, and **3I**.

^{1}H NMR spectrum of 22 compounds exhibited only one signal for the 5-methylidene proton in the range from 7.73 to 7.78 ppm in dimethylsulfoxide (DMSO)-d_6 solution, at lower field values than those expected for the *E*-isomers.[21,22] The *Z*-configuration of similar compounds also have been identified from the ^{1}H-coupled ^{13}C NMR spectrum and X-ray data followed by examination of the splitting pattern and coupling constant of the signal of carbonyl group in the heterocyclic system.[23−25] These experiments confirmed *Z*-configuration of similar compounds, which can be assumed for our compounds.

At this stage, the products were fully analyzed and characterized by ^{1}H-nuclear magnetic resonance (NMR), mass spectrometry (MS), and high-performance liquid chromatography (HPLC) before entering the biological screening.

RESULTS AND DISCUSSION

Inhibition of NO Production in RAW 264.7 Microphages. We initially accessed the capacity of our targeted compounds contained thiazolidine-2,4-dione to inhibit NO production. Here indomethacin (Figure 1),[26] as a nonsteroidal anti-inflammatory drug, was chosen as a positive control. As depicted in Table 1, four compounds (**3I**, **3M**, **3O**, and **3U**) suppressed the LPS-induced production of NO at a concentration of 10 μM and their inhibitory rates (IR) were all more than 70% compared to indomethacin (IR = 63.2%). Among them, **3I** (IR = 80.9%) and **3U** (IR = 83.9%) showed the most potent inhibitory effects.

dx.doi.org/10.1021/jm1011534 |*J. Med. Chem.* 2011, 54, 2060–2068

Table 1. Inhibitory Effects of 3A−V on NO Production in RAW 264.7 Cells[a]

compds	NO inhibition (%) ± SD	compds	NO inhibition (%) ± SD
indomethacin	63.2 ± 4.0[c]	**3L**	10.0 ± 3.1
3A	55.3 ± 11.1[b]	**3M**	72.0 ± 2.1[c]
3B	38.4 ± 1.8[b]	**3N**	36.0 ± 3.8
3C	0.6 ± 9.7	**3O**	83.9 ± 1.3[d]
3D	16.2 ± 6.2	**3P**	51.0 ± 5.4[b]
3E	26.6 ± 2.9	**3Q**	47.8 ± 1.2[b]
3F	10.2 ± 1.9	**3R**	41.6 ± 3.3[b]
3G	41.5 ± 3.1[b]	**3S**	14.6 ± 4.1
3H	57.9 ± 2.0[b]	**3T**	12.5 ± 6.2
3I	80.9 ± 5.0[c]	**3U**	70.9 ± 13.6[c]
3J	9.7 ± 5.4	**3 V**	45.1 ± 3.7[b]
3K	23.7 ± 3.2		

[a] RAW 264.7 cells were pretreated with **3A−V** at the concentration of 10 μM for 2 h and then incubated with LPS (1 μg/mL) for 18 h. The amount of nitrite with LPS-treated only group was set as 100.0% and the vehicle control as 0.0%. Inhibition (%) = [LPS (OD_{540}) − compounds (OD_{540})]/[LPS (OD_{540}) − control (OD_{540})] × 100. Results are means ± SD of at least three independent experiments. [b] $P < 0.05$. [c] $P < 0.01$. [d] $P < 0.001$ versus the LPS-treated group.

Compared to the unsubstituted phenyl ring compound **3A**, the inhibitory potency decreased dramatically when para substituents of electron-donating groups (methyl for **3B**, methoxyl for **3C**, trifluoromethyl for **3E**, and *meta*- or *para*-dimethoxy for **3D**) were added, and then, para substituents of electron-withdrawing groups (acetyl for **3F** and *para*-halogenation including chlorine and bromine atom for **3J**−**L** and **3N**) have clear negative effects on inhibitory potency. However, the fluorine atom at the para position (*para*-fluorinated for **3H** and *meta*-, *para*-difluorinated for **3O**) improved the inhibitory effects as a result of their inherent electronegativity and small atomic radius. The properties may contribute to the stability and also served to block metabolism at particularly reactive sites and reduced metabolism of the aromatic group by decreasing its electron density. Our results on inhibitory activity of NO production indicated that the introduction of *meta*-halogenated groups was relevant, as **3G** and **3I** showed more activity than the analogues **3H** and **3J**.

We also examined the replacement of phenyl ring (**3A**) with pyridin-2-yl (compound **3S**) and 5-methyl pyridine-2-yl (compound **3T**) group, the potency of inhibition decreased. The presence of hydrophilic group seemed to reduce the capacity of inhibition on NO production. Inclusion of flexible cyclohexyl (**3Q**) and benzyl (**3R**) substituent resulted in a little reduction in potency and were essentially equipotent with the activity of **3A**. Introducing of the steric bulk of α- and β-naphthalene also improved the inhibition, especially compound **3U** (IR = 70.9%).

Inhibition of iNOS Activity, PEG_2 Production, and Cytotoxicity. Four compounds (**3I**, **3M**, **3O**, and **3U**) were exposed to RAW 264.7 cells to investigate the inhibitory effects on iNOS activity, the production of iNOS-mediated NO, COX-2-derived PGE_2, and cytotoxicity. As shown in Table 2, the four compounds possessed remarkable inhibitory activity on iNOS, PEG_2, and NO. As anticipated, **3I** exhibited the most potent inhibitory potencies on iNOS activity (IC_{50} = 8.66 μM), the generation of iNOS-mediated NO and COX-2-derived PGE_2 (IC_{50} = 4.16 and 23.55 μM, respectively) compared to indomethacin (IC_{50} = 15.37 μM for iNOS, 15.37 μM for NO, and 48.59 μM for PGE_2) on LPS-induced RAW 264.7 cells. To check whether the suppressive effects of the four compounds on iNOS, NO, and PEG_2 was related to cell viability, MTT assay was adopted. The most potent one, **3I**, showed no cytotoxicity on RAW 264.7 microphages (without or with LPS, IC_{50} > 100 μM). However, we found that effects of **3U** (IC_{50} = 62.26 μM without LPS and 54.97 μM with LPS) were more cytotoxic than the other three compounds, **3M** and **3U** were less potent than **3I**. On the basis of cellular viability and anti-inflammatory activity in vitro, **3I** were further evaluated in the next experimental process.

Docking Study of All Molecules with Murine iNOS. All molecules were docked to the active site of murine iNOS by the aid of a protein−ligand docking program FRED. Compounds **3I**, **3M**, and **3U** are among the top five structures by computational scoring which almost are consistent with our in vitro screenings. As the most potent molecule **3I**, its interaction mode binding to iNOS protein data was depicted in Figure 2. The *meta*-chlorophenyl moiety of **3I** was buried in a pocket wove by Pro344 and Ph363-Tyr367. The linker between the two phenyl groups was enclosed by a polar cavity consisting of Gln257, Val346, and Glu371. The thiazolidinedione moiety was surrounded by Trp457, Met114, Ans115, Tyr485, and Ans348. In addition, two strong hydrogen bonds are formed between **3I** and Glu371 and Asn115 and a $\pi-\pi$ interaction between the hetero pentacycle of **3I** and the side chain of Tyr485 was also observed. These computational results confirmed our hypothesis that **3I** was a potent and potential iNOS inhibitor with perfect binding to the active site of murine iNOS, and the hypothesis would be tested by Western blot analysis further. The docking results of all molecules binding to iNOS protein were shown in Supporting Information.

Detection of iNOS and COX-2 Expression. Because the high level of NO is mainly generated by iNOS, the expression of iNOS protein is an important step during the process of LPS-activated production.[28] To investigate the **3I**-activated signaling pathway and verify the docking result of **3I** binding to murine iNOS, Western blot analysis was applied to evaluate the effects on expression of iNOS protein. As shown in Figure 3, the expression of iNOS and protein were significantly inhibited by **3I** in a good dose-dependent manner (0−24 μM). Furthermore, COX-2 is inducible and leads to excess production of prostaglandin (such as PEG_2) during injury, resulting in pain and inflammation.[29] The inhibition of COX-2 protein is also thought to be enough to provide the anti-inflammatory activity. Our result displayed that the expression of COX-2 protein also was remarkably suppressed by **3I** at concentrations of 12 and 24 μM. Therefore, the data demonstrated that **3I** inhibited NO and PEG_2 production through down-regulation of LPS-induced iNOS and COX-2.

Treatment of Acute Inflammation. To evaluate the In Vivo anti-inflammatory potency of **3I**, two animal models of acute inflammation were employed including carrageenan-induced paw edema test and acetic acid-induced vascular permeability test. The edema is an important parameter of acute inflammation for evaluating compounds with potential anti-inflammatory activity. In the carrageenan-induced paw edema test, the inflammatory response was quantified by increment in paw size (edema) 2 h after carrageenan was injected and the paw edema was observed. Oral administrations of **3I** at doses of 10 and 50 mg/kg inhibited carrageenan-induced paw edema (Figure 4A). Treatment with 50 mg/kg **3I** exhibited more inhibitory activity than dose of 10 mg/kg and **3I** suppressed edema formation after edema induction with the inhibitory rate of 36.2%. Indomethacin

Table 2. IC_{50} Values on NO, iNOS, PEG_2, and Cytotoxicity in RAW 264.7 Cells[a]

				cytotoxicity IC_{50} (μM)	
compds	NO IC_{50} (μM)	iNOS IC_{50} (μM)	PEG_2 IC_{50} (μM)	without LPS	with LPS
indomethacin	48.89	23.47	15.37	>100	>100
3I	23.55	8.66	4.16	>100	>100
3M	57.42	26.13	14.81	>100	>100
3O	34.08	13.92	7.12	62.26	54.97
3U	40.00	20.87	16.12	>100	>100

[a] Cytotoxicity = (1 − [compounds (OD_{570}) − background (OD_{570})]/[control (OD_{570}) − background (OD_{570})]) × 100%.

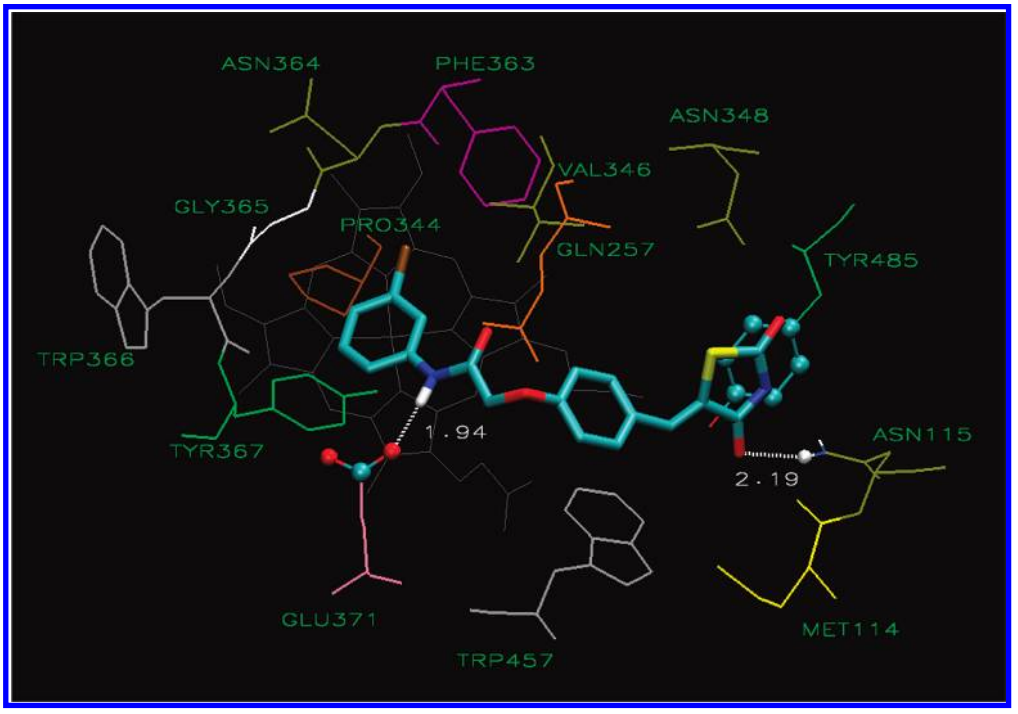

Figure 2. The interaction mode of **3I** within the active site of murine iNOS (PDB ID: 1r35). Residues in the active site are displayed in line style and colored differently. Human erythrocyte membrane protein (HEM) is depicted by gray line and **3I** is represented with stick. Hydrogen bonds and $\pi-\pi$ interaction formed between residues within the active site and **3I** are highlighted. This figure was generated by the software Virtual Molecular Dynamics (VMD).[27]

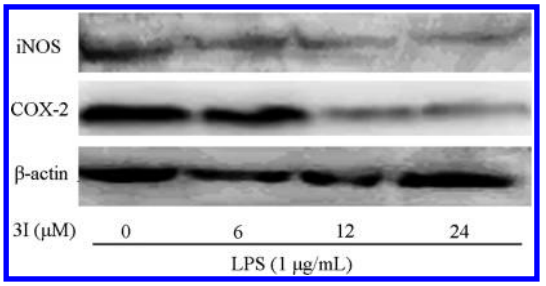

Figure 3. Effect of **3I** on LPS-induced iNOS and COX-2 protein expression in RAW 264.7 cells. RAW 264.7 cells were pretreated with the indicated concentrations of **3I** for 2 h and treated with LPS (1 μg/mL) for 18 h. Equal amounts of total protein were subjected to 8% (iNOS and COX-2) SDS-PAGE.

showed an inhibitory rate of 33.3−40.7% of edema development. However, unsatisfactory results of **3I**-treated rats on inhibition of vascular permeability were obtained in contrast to rats' access to indomethacin in acetic acid-induced vascular permeability test (Figure 4B). As suggested above, the consequences of the two inflammatory models indicated that **3I** was a potential anti-inflammatory agent on inhibition of inflammatory edema.

Treatment of Adjuvant-Induced Arthritis. Because it inhibited the carrageen in paw edema, **3I** has been chosen to be examined on adjuvant-induced arthritis (AIA). AIA is a well-established experimental model of rheumatoid arthritis and is often used for testing agents for anti-inflammatory activity. In this model, 90−100% of rats developed arthritis within 14−18 days after adjuvant injection. Histological changes, including leukocyte (mainly neutrophil) invasion and synovial cell activation, precede clinical symptoms. As displayed in Figure 5A, rats treated with **3I** at a dose of 50 mg/kg did not develop severe arthritis, indicating that it exhibited potential immune- modulating activity. Arthritic score and body weight loss were significantly reduced in the therapeutic process. The time course of adjuvant arthritic development, expressed as arthritic scores, was shown in Figure 5A. A continuous joint swelling was observed in the hind limbs and AIA rats had

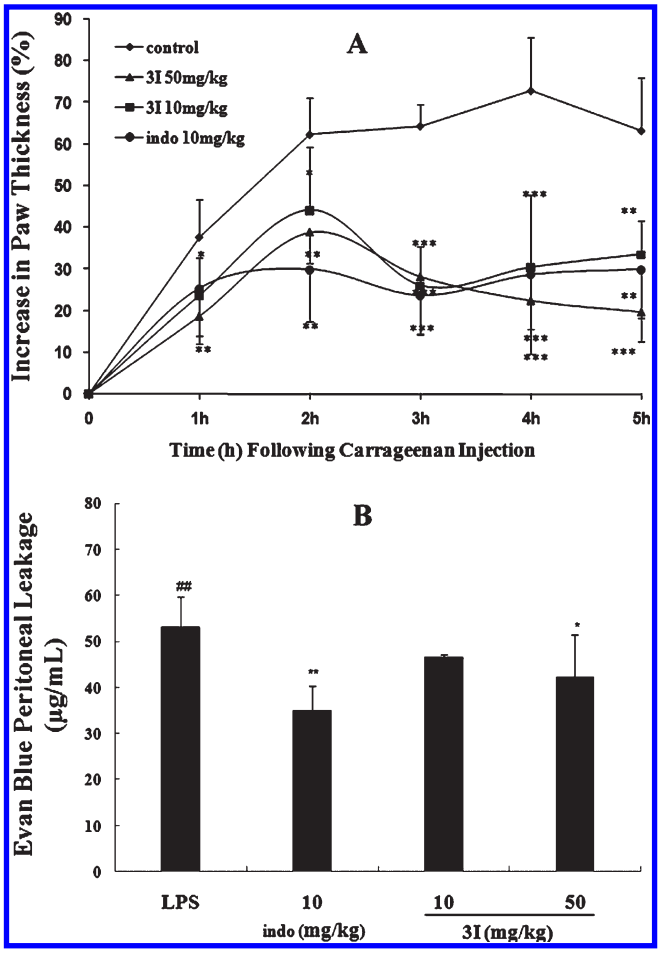

Figure 4. Effect of **3I** on two animal models of inflammation. (A) Carrageenan-induced paw edema in ICR mice. (B) Acetic acid-induced vascular permeability in ICR mice. Indo, indomethacin as a positive control. The results were expressed as the means ± SD ($n = 6$). $^{\#\#}P < 0.001$ versus blank. $^{*}P < 0.05$; $^{**}P < 0.01$; $^{***}P < 0.001$ versus vehicle control.

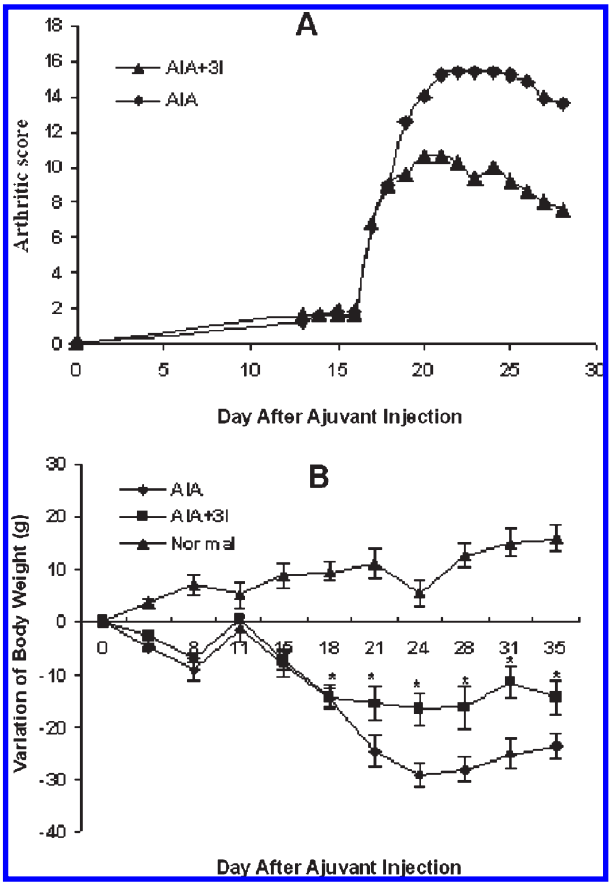

Figure 5. Effect of **3I** on AIA model. **3I** was orally administered once daily at a dose of 50 mg/kg. (A) Clinical disease activity score of **3I**. (B) Body weight after adjuvant injection. The results were expressed as the means ± SD ($n = 6$). $^{*}P < 0.05$ versus vehicle control.

higher arthritic scores than those treated with **3I** between days 17 and 28. **3I** were found to improve the body weight loss and the percent of variation was 15.1% (Figure 5B).

From the results of H&E staining (Figure 6), massive leukocytes infiltrated into the synovial tissue and synovial fluid of joints with the appearance of synovial cell proliferation in AIA model group while treatment with **3I** at the dosed of 50 mg/kg was observed with few signs of inflammation and revealed substantial improvements in histological state of joints.

Having identified potent anti-inflammatory agent with favorable in vitro and in vivo results, we selected **3I** for further profiling in rat pharmacokinetics (Table 3). The pharmacokinetic data of **3I** exhibited that the oral bioavailability was 18.10%, with the half-time of 2.16 h.

CONCLUSION

Inflammation is a host response to stimuli and is characterized by the signs of redness, swelling, heat, and pain. The pathology of inflammation is initiated by complex processes caused by pathogens such as LPS, which is a prototypical endotoxin.[30] LPS activate directly macrophages to produce proinflammatory cytokines, such as NO, TNF-α, and IL-1β.[31] Therefore, pharmacological reduction of LPS-inducible inflammatory mediators (e.g., NO, TNF-α, and IL-1β) is regarded as one of the essential conditions to alleviate a variety of inflammatory diseases triggered by activation of macrophages.

In this study, we have identified that **3I** effectively suppressed the iNOS activity, the production of iNOS-mediated NO, and COX-2-derived-PEG_2 in RAW 264.7 cells induced by LPS. **3I** also inhibited the expression of iNOS and COX-2 protein. Furthermore, we investigated anti-inflammatory activity of **3I** in mouse model of acute and chronic inflammation. For acute inflammatory models in ICR mice, treatment of **3I** improved the inflammatory response such as decrement of the paw edema. In an adjuvant-induced arthritis rat model, oral administration (50 mg/kg) of **3I** resulted in significant reduction of foodpad swelling and improvement of pathology from joints of rats. These observations suggest that **3I** might be an effective agent for the treatment of inflammatory diseases.

EXPERIMENTAL SECTION

Materials. LPS (*Escherichia coli* serotype 0111:B4), MTT, Evans blue, Carrageenan from seaweed (a mixture of λ- and κ-carrageenans), incomplete Freund's adjuvant (IFA), and indomethacin were obtained from Sigma Chemical Co. (St. Louis, MO). The enzyme immunoassay (EIA) kits for PGE_2, TNF-α, and IL-1β were purchased from R&D Systems (Minneapolis, MN). iNOS rabbit polyclonal antibody (1:1000) and β-actin monoclonal antibody (1:1000) were obtained from Cell

dx.doi.org/10.1021/jm1011534 |*J. Med. Chem.* 2011, 54, 2060–2068

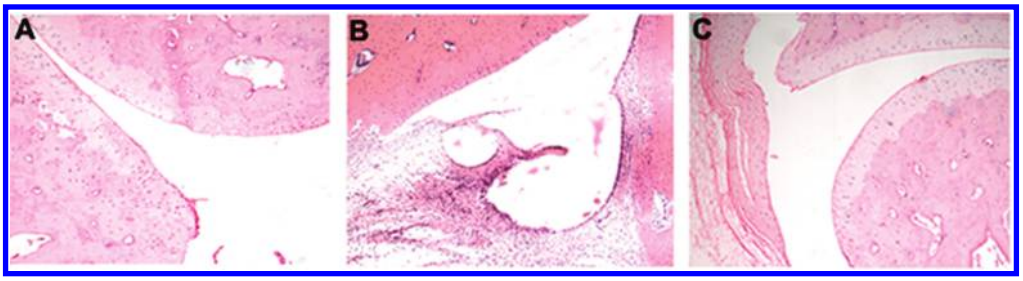

Figure 6. H&E staining for histological changes of joints of **3I**-treated AIA rats. (A) Normal. (B) Model. (C) **3I**-treated model group at the dose of 50 mg/kg.

Table 3. Pharmacokinetic Profiles for 3I in SD Rats[a]

	C_{max} (μM)	T_{max} (h)	$AUC_{0-t\ h}$ (μM·h/L)	$t_{1/2}$ (hr)	F (%)
po	15.31	0.18	10.0	2.16	18.10
iv	27.0	0.08	11.05	0.28	

[a] Dose: 50 mg/kg, po; 10 mg/kg, iv.

Signaling Technology, Inc. (Beverly, MA). ICR male mice weighing 18−25 g and female inbred Lewis rats (6−8 weeks old) were purchased from Tengxin Biotech Company (Chongqing, P. R. China).

Cell Culture. RAW 264.7 murine macrophages were obtained from American Type Culture Collection (ATCC, Rockville, MD, USA). These cells were grown in RPMI 1640 containing 10% FBS, 100 units/mL penicillin, and 100 μg/mL streptomycin in a 95% air, 5% CO_2 humidified atmosphere at 37 °C.

Nitrite Assay. RAW 264.7 cells were seeded into a 96-well culture plate at a density of 1×10^4 cells per well with 500 μL of culture medium and incubated for 24 h. The cells were then pretreated with compounds (**3A**−**V**) at a concentration of 10 μg/mL or compounds **3I**, **3M**, **3O**, **3U**, and indomethacin with a series of concentrations for 2 h before stimulation with LPS (1 μg/mL) for 18 h. The nitrite concentration in the medium was measured according to the Griess reaction by adding 50 μL of Griess reagent (1% sulfanilamide and 0.1% *N*-(1-naphthyl)ethylenediamine dihydrochloride in 5% phosphoric acid) to 50 μL of medium for 5 min. The optical density at 540 nm (OD_{540}) was measured with a microplate reader. Concentrations were calculated by comparison with the OD_{540} values of a standard solution of sodium nitrite prepared in culture medium.

Cell Cytotoxicity. Cell cytotoxicity was evaluated by MTT and expressed as IC_{50}. Raw 264.7 cells were treated with compounds alone or in combination with LPS for 24 h. Cells were washed with PBS and incubated in 0.5 mg/mL MTT reagent dissolved in RPMI 1640 for 4 h, and the formazan product dissolved in 150 μL of DMSO. The optical density was measured using an ELISA plate reader at 570 nm (OD_{570}).

Assay of iNOS Enzymatic Activity. After treated with LPS (1 μg/mL) and indomethacin, **3I**, **3M**, **3O**, and **3U** (1−50 μM) for 2 h at 37 °C, the culture supernatant was removed and 100 μL of NOS assay buffer (1×) were added to each well. Then 100 μL of NOS assay reaction solution (50% NOS assay buffer, 39.8% Milli-Q water, 5% L-arginine solution, 5% 0.1 mM NADPH, 0.2% DAF-FMDA) was added to each well and incubated for 2 h at 37 °C. Fluorescence was measured with a fluorescence plate reader (Biotek) at excitation of 485 nm and emission of 528 nm.

Determination of PGE_2. RAW 264.7 cells were seeded in wells and incubated for 24 h. After incubation, the cells were incubated with compounds (**3I**, **3O**, **3M**, and **3U**) of different concentrations in the presence of LPS (1 μg/mL) for 24 h. The PGE_2 concentration in the culture medium was determined by ELISA kit (R&D Systems, Minneapolis, MN).

Detection of iNOS and COX-2 Expression. After the treatment with LPS (1 μg/mL) and **3I** (0−24 μM), cells were washed three times with PBS and were lysed by 30 min incubation on ice in lysis buffer containing 10 mM Tris-Cl, pH 7.4, 3 mM $CaCl_2$, 2 mM $MgCl_2$, 1% NP-40, 0.5 mM phenylmethylsulfonyl fluoride (PMSF), and protease inhibitor cocktail. The lysate was centrifuged at 15000*g* for 10 min and the supernatant was collected. The protein concentration was determined using the Bio-Rad protein assay reagent (Bio-Rad, Hercules, CA). Total protein equivalents were separated by 8% SDS-polyacrylamide gel electrophoresis (SDS-PAGE) and were electroblotted onto polyvinylidene difluoride (PVDF) membrane. The transblotted membrane was washed twice with TBST. After blocking with TBST containing 5% skim milk for 2 h, the membrane was properly cut into three membranes corresponding to iNOS, COX-2, and β-actin. The membranes were incubated overnight with primary antibodies from rabbit or mouse at 4 °C with gentle shaking. Blots were washed three times in TBST for 30 min, followed by incubation with horseradish peroxidase (HRP)-conjugated secondary antibody for 40 min at room temperature. Immunoreactive bands were visualized by the enhanced chemiluninescence system.

In Vivo Experiments. ICR male mice and female Lewis rats were housed in filtered-capped polycarbonate cages and allowed food and water ad libitum. Animals were kept on a cycle of 12 h light/darkness at 22 ± 1 °C and acclimated for at least one week until use. All progressions were maintained under controlled conditions and animals received human care according to National Institutes of Health Guidelines before and during experiment.

Carrageenan-Induced Paw Edema Test in ICR Mice. The mice were randomly divided into four groups. Doses (10 mg/kg and 50 mg/kg) of compound **3I** were administered ip to the test groups, respectively. The positive control group and the vehicle control group were given access to indomethacin (10 mg/kg, ip) and the same volume of olive oil (10 mL/kg, ip), respectively. Thirty minutes after the administration, acute paw edema was induced in the right hind paw by subplantar injection of 1% freshly prepared carrageenan suspension in normal saline, 0.05 mL per mouse. The thickness of the paw was measured preinjection and at intervals of 1, 2, 3, 4, and 5 h postinjection, using a dial thickness gauge. The percent increase of paw thickness was calculated based on the preinjection thickness of the paw.

Acetic Acid-Induced Vascular Permeability Test in ICR Mice. The mice were randomly divided into four groups. Doses (10 and 50 mg/kg) of compound **3I** were administered ip to the test groups, respectively. The positive control group and the vehicle control group were given access to indomethacin (10 mg/kg, ip) and the same volume of olive oil (10 mL/kg, ip), respectively. After 30 min, 10 mL/kg body weight of 1% Evans blue in normal saline was injected intravenously into the tail vein of each animal. Sixty minutes after administration, each mouse was injected with 10 mL/kg (ip) of 1.2% acetic acid in normal saline. Fifty minutes after the injection, the mice were sacrificed by cervical dislocation. Eight milliliters of normal saline was injected into the peritoneal cavity, and the washing solutions were collected in test tubes. To clear turbidity due to protein, 1 N NaOH solution to a ratio of 0.1 mL/10 mL was added to each tube, and allowed to stand overnight at

dx.doi.org/10.1021/jm1011534 |*J. Med. Chem.* 2011, 54, 2060–2068

4 °C. The solution was subjected to colorimetry using a UV/vis spectrophotometer GeneQuant II (Amersham Bioscience, Sweden) at 610 nm. The vascular permeability effects were expressed according to the concentration of dye (μg/mL) that had leaked into the peritoneal cavity.

Induction and Evaluation of Adjuvant-Induced Arthritis. The rat AIA model was introduced in this experiment. The rats were injected subcutaneously (sc) at the tail base with 0.5 mg heat-killed inactivated *Mycobacterium tuberculosis* emulsified in 0.1 mL IFA on day 0, at multiple sites. **3I** was orally administered once daily at a dose of 50 mg/kg, an effective dose according to the previous two animal models of inflammation experiments. The treatment was initiated from the onset of disease on day 17 after the vaccination. Animals from the control group received 0.5% polysorbate 80 only. All animals were treated continuously up to day 28.

Body weight of rats was observed thrice daily after adjuvant injection. The clinical disease activity score was initiated from day 13 and assessed as follows: the animals were inspected every day for symptoms of clinical arthritis. The score for each limb ranged from **0** to **4**; **0**, no arthritis; **1**, redness or swelling of one toe/finger joint; **2**, redness and swelling of more than one toe/finger joints; **3**, involvement of the ankle and tarsal-metatarsal joints; **4**, redness or swelling of the entire paw. The clinical score was calculated by adding the scores for four individual legs.

Histopathological Evaluation. Rats were all sacrificed on day 28. The legs reserving knee joints were removed in toto, fixed in 10% formalin, decalcified in EDTA buffer, subjected in a series progression of dehydration, and then embedded in paraffin. Samples were serially sectioned at 4 μm and processed routinely for H&E staining. The histological changes were examined under microscope.

Pharmacokinetic Study of 3I. Two groups of male and female Sprague−Dawley rats (180−200 g) were fasted overnight and received compound **3I** as an intravenous (IV) dose (10 mg/kg) or by oral gavage (50 mg/kg, Dissolved into Tween 80). Blood samples (0.5 mL) were obtained retro-orbital bleeding at 0.05, 0.25, 0.5, 1, 3, 6, 8, and 24 h post dose for the IV group and at 0.25, 0.5, 1, 3, 6, 8, and 24 h post dose for the PO dose group. At each time point, three mice were bled resulting in a composite pharmacokinetic profile. The tubes were inverted several times to ensure mixing and placed on ice. Plasma was obtained following centrifugation at 4 °C (1500−2000*g*). Plasma samples were stored at − 20 °C until analysis by a UPLC assay.

Chemistry. Chemical reagents of analytical grade were purchased from Chengdu Changzheng Chemical Factory (Sichuan, P. R. China). The final compounds were synthesized using an EYELA personal organic synthesizer with ChemiStation PPS-CTRL and PPW-20A (Tokyo, Rikakikai) using a 5-well liquid-phase reaction block. TLC was performed on 0.20 mm silical gel 60 F_{254} plates (Qingdao Ocean Chemical Factory, Shangdong, China). ^{1}H NMR were recorded at 400 MHz on a Varian spectrometer (Varian, Palo Alto, CA, USA) model Gemini 400 and reported in parts per million. Chemical shifts (δ) are quoted in ppm relative to tetramethylsilane (TMS) as an internal standard, where (δ) TMS = 0.00 ppm. The multiplicity of the signal is indicated as s, singlet; d, doublet; t, triplet; q, quartet; m, multiplet, defined as all multipeak signals where overlap or complex coupling of signals makes definitive descriptions of peaks difficult. MS were measured by Q-TOF Priemier mass spectrometer utilizing electrospray ionization (ESI) (Micromass, Manchester, UK). Room temperature (RT) is within the range 20−25 °C. The purity of compound screened in biological assays was determined to be ≥97% by HPLC analysis with a phodediode array detector (Waters, Milford, MA, USA) and the chromatographic column was a atlantis C_{18} (150 mm × 4.6 mm, I.D. 5 μm) (Waters, Milford, Ireland). All compounds were supplied as 1 mg/mL in DMSO or methanol with 10 μL injected on a partial loop fill at a flow rate of 1 mL/min for 30 min. Solvent A, 75% methanol; Solvent B, 25% water with 0.5% trifluoroacetic acid. The detailed HPLC analysis of **3A**−**V** were shown in the Supporting Information.

General Procedure for Synthesis of 2-Chloro-*N*-substituted-acetamide (1A−V). 2-Chloroacetyl chloride (24 mmol) was slowly added dropwise to a mixture of R-NH_2 (20 mmol) and Et_3N (24 mmol, 3.3 mL) in anhydrous CH_2Cl_2 (20 mL) at 0 °C. The reaction mixture was warmed to room temperature and stirred for an additional 20 h. After the solvent was removed under reduced pressure, the residue was washed with ice water (3 × 20 mL), and the precipitate was separated by filtration. The crude product was purified by crystallization from a mixture solvent of Ether/petroleum.

General Procedure for Synthesis of 2-(4-Formylphenoxy)-*N*-substituted-phenyl-acetamide and Special Aldehyde Intermediates (2A−V). 4-Hydroxybenzaldehyde (1.34 g, 11 mmol), anhydrous K_2CO_3 (2.76 g, 20 mmol), and the 2-chloro-*N*-substituted-acetamide (10 mmol) were dissolved in anhydrous acetone (30 mL), and then KI (166 mg, 1 mmol) were added into the solution. The reaction mixture was refluxed for 24 h and then cooled to room temperature. Then the K_2CO_3 solid was filtered and the acetone solution was removed under reduced pressure to obtain the crude products. The residue was purified by silica gel column chromatography (eluent:ethyl acetate/petroleum = 1/1.5) to give the appropriate aldehyde product.

General Procedure for Synthesis of 3A−V. The appropriate aldehyde (3.0 mmol), 10 mL glacial acetic acid, β-alanine (6.0 mmol), and 2-thiazolidin-4-one (6.0 mmol) were mixed in parallel in 12 test tubes with reflux condensers and refluxed at 1000 rpm in tubes for 4 h. Then a small portion of water was added, and the precipitated solids were collected by sucking filtration and washed with glacial acetic acid (3 × 15 mL), distilled water (4 × 15 mL), and ether (2 × 10 mL). The solids obtained were dried in vacuum at 40 °C for 24 h.

(*Z*)-2-(4-((2,4-Dioxothiazolidin-5-ylidene)methyl)phenoxy)-*N*-phenylacetamide (3A). Yield 83.4%; analytical HPLC purity = 98.60%; light-yellow solid. ^{1}H NMR (400 MHz, DMSO-d_6): δ 12.54 (s, 1H), 10.15 (s, 1H), 7.76 (s, 1H), 7.64−7.58 (m, 4H), 7.33 (t, 2H, J = 8.2 Hz), 7.15 (d, 2H, J = 8.4 Hz), 7.09 (t, 1H, J = 7.4 Hz), 4.81 (s, 2H). MS (ESI), m/z: 354.07 $[M - H]^-$.

(*Z*)-2-(4-((2,4-Dioxothiazolidin-5-ylidene) methyl) phenoxy)-*N*-*p*-tolylacetamide (3B). Yield 74.3%; analytical HPLC purity = 98.24%; light-yellow solid. ^{1}H NMR (400 MHz, DMSO-d_6): δ 12.54 (s, 1H), 10.06 (s, 1H), 7.76 (s, 1H), 7.59 (d, 2H, J = 8.8 Hz), 7.51 (d, 2H, J = 8.4 Hz), 7.14 (t, 4H, J = 9.2 Hz), 4.78 (s, 2H), 2.26 (s, 3H). MS (ESI), m/z: 367.18 $[M - H]^-$.

(*Z*)-2-(4-((2,4-Dioxothiazolidin-5-ylidene)methyl)phenoxy)-*N*-(4-methoxyphenyl)acetamide (3C). Yield 87.9%; analytical HPLC purity = 98.54%;. light-yellow solid. ^{1}H NMR (400 MHz, DMSO-d_6): δ 12.54 (s, 1H), 10.01 (s, 1H), 7.76 (s, 1H), 7.59 (d, 2H, J = 8.4 Hz), 7.53 (d, 2H, J = 8.8 Hz), 7.16 (d, 2H, J = 8.4 Hz), 6.90 (d, 2H, J = 4.8 Hz), 4.77 (s, 2H), 3.72 (s, 3H). MS (ESI), m/z: 383.10 $[M - H]^-$.

(*Z*)-*N*-(3,4-Dimethoxyphenyl)-2-(4-((2,4-dioxothiazolidin-5-ylidene)methyl)phenoxy)acetamide (3D). Yield 86.3%; analytical HPLC purity = 99.05%; yellow solid. ^{1}H NMR (400 MHz, DMSO-d_6): δ 12.54 (s, 1H), 10.00 (s, 1H), 7.76 (s, 1H), 7.59 (d, 2H, J = 7.6 Hz), 7.33(d, 1H, J = 2.0 Hz), 7.18−7.15 (m, 3H), 6.90 (d, 1H, J = 8.8 Hz), 4.77 (s, 2H), 3.72 (s, 3H), 3.72 (s, 3H). MS (ESI), m/z: 413.10 $[M - H]^-$.

(*Z*)-2-(4-((2,4-Dioxothiazolidin-5-ylidene)methyl)phenoxy)-*N*-(4-(trifluoromethyl)phenyl)acetamide (3E). Yield 75.8%; analytical HPLC purity = 98.78%; yellow solid. ^{1}H NMR (400 MHz, DMSO-d_6): δ 12.53 (s, 1H), 10.52 (s, 1H), 7.85 (d, 2H, J = 8.0 Hz), 7.75 (s, 1H), 7.70 (d, 2H, J = 8.4 Hz), 7.58 (d, 2H, J = 8.8 Hz), 7.15 (d, 2H, J = 8.8 Hz), 4.85 (s, 2H). MS (ESI), m/z: 421.01 $[M - H]^-$.

(*Z*)-*N*-(4-Acetylphenyl)-2-(4-((2,4-dioxothiazolidin-5-ylidene)methyl)phenoxy)acetamide (3F). Yield 84.0%; analytical HPLC purity = 99.10%; yellow solid. ^{1}H NMR (400 MHz, DMSO-d_6): δ 12.53 (s, 1H), 10.50 (s, 1H), 7.95 (d, 2H, J = 8.4 Hz), 7.77 (d, 1H,

J = 10.8 Hz), 7.76 (s, 2H), 7.59 (d, 2H, J = 8.4 Hz), 7.16 (d, 2H, J = 8.4 Hz), 4.86 (s, 2H), 2.53 (s, 3H). MS (ESI), m/z: 395.26 [M − H]$^-$.

(*Z*)-2-(4-((2,4-Dioxothiazolidin-5-ylidene)methyl)phenoxy)-*N*-(3-fluorophenyl)acetamide (3G). Yield 73.7%; analytical HPLC purity = 99.11%; white solid. ^{1}H NMR (400 MHz, DMSO-d_6): δ 12.53 (s, 1H), 10.33 (s, 1H), 7.83 (s, 1H), 7.75 (s, 1H), 7.58 (d, 2H, J = 8.4 Hz), 7.52 (d, 1H, J = 8.4 Hz), 7.36 (t, 1H, J = 8.0 Hz), 7.15 (d, 3H, J = 8.4 Hz), 4.82 (s, 2H). MS (ESI), m/z: 371.01 [M − H]$^-$.

(*Z*)-2-(4-((2,4-Dioxothiazolidin-5-ylidene)methyl)phenoxy)-*N*-(4-fluorophenyl)acetamide (3H). Yield 71.8%; analytical HPLC purity = 99.40%; yellow solid. ^{1}H NMR (400 MHz, DMSO-d_6): δ 12.54 (s, 1H), 10.21 (s, 1H), 7.76 (s, 1H), 7.67−7.63 (m, 2H), 7.59 (d, 4H, J = 8.8 Hz), 7.17 (t, 2H, J = 8.4 Hz), 4.80 (s,2H). MS (ESI), m/z: 372.06 [M − H]$^-$.

(*Z*)-*N*-(3-Chlorophenyl)-2-(4-((2,4-dioxothiazolidin-5-ylidene)methyl)phenoxy)acetamide (3I). Yield 92.8%; analytical HPLC purity = 98.53%; white solid. ^{1}H NMR (400 MHz, DMSO-d_6): δ 12.55 (s, 1H), 10.35 (s, 1H), 7.84 (s, 1H), 7.77 (s, 1H), 7.59 (d, 2H, J = 8.4 Hz), 7.53 (d, 1H, J = 8.0 Hz), 7.37 (t, 1H, J = 8.2 Hz), 7.16 (d, 2H, J = 8.4 Hz), 4.83 (s, 2H). MS (ESI), m/z: 386.98 [M − H]$^-$.

(*Z*)-*N*-(4-Chlorophenyl)-2-(4-((2,4-dioxothiazolidin-5-ylidene)methyl)phenoxy)acetamide (3J). Yield 73.4%. analytical HPLC purity = 98.06%; yellow solid. ^{1}H NMR (400 MHz, DMSO-d_6): δ 12.54 (s, 1H), 10.30 (s, 1H), 7.76 (s, 1H), 7.67 (m, 2H, J = 8.8 Hz), 7.59 (d, 2H, J = 8.8 Hz), 7.39 (d, 2H, J = 9.2 Hz), 7.16 (d, 2H, J = 8.8 Hz), 4.81 (s,2H). MS (ESI), m/z: 387.06 [M − H]$^-$.

(*Z*)-*N*-(4-Bromophenyl)-2-(4-((2,4-dioxothiazolidin-5-ylidene)methyl)phenoxy)acetamide (3K). Yield 80.2%; analytical HPLC purity = 99.45%; light-yellow solid. ^{1}H NMR (400 MHz, DMSO-d_6): δ 12.53 (s, 1H), 10.29 (s,1H), 7.76 (s, 1H), 7.62−7.57 (m, 4H), 7.51 (d, 2H, J = 8.8 Hz), 7.15 (d, 2H, J = 8.8 Hz), 4.841 (s, 2H). MS (ESI), m/z: 431.08 [M − H]$^-$.

(*Z*)-*N*-(2,4-Dichlorophenyl)-2-(4-((2,4-dioxothiazolidin-5-ylidene)methyl)phenoxy)acetamide (3L). Yield 80.3%; analytical HPLC purity = 98.16%; light-yellow solid. ^{1}H NMR (400 MHz, DMSO-d_6): δ 12.55 (s, 1H), 9.81 (s, 1H), 7.84−7.80 (m, 1H), 7.77 (s, 1H), 7.72−7.71 (m, 1H), 7.60 (d, 2H, J = 8.8 Hz), 7.47−7.44 (m, 1H), 7.18 (d, 2H, J = 8.8 Hz), 4.89 (s, 2H). MS (ESI), m/z: 421.10 [M − H]$^-$.

(*Z*)-*N*-(3,5-Dichlorophenyl)-2-(4-((2,4-dioxothiazolidin-5-ylidene)methyl)phenoxy)acetamide (3M). Yield 72.1%; analytical HPLC purity = 98.64%; light-yellow solid. ^{1}H NMR (400 MHz, DMSO-d_6): δ 12.55 (s, 1H), 10.47 (s, 1H), 7.77 (s, 1H), 7.74 (d, 2H, J = 1.6 Hz), 7.59 (d, 2H, J = 9.2 Hz), 7.33 (t, 1H, J = 1.6 Hz), 7.16 (d, 2H, J = 8.8 Hz), 4.84 (s, 2H). MS (ESI), m/z: 421.01 [M − H]$^-$.

(*Z*)-*N*-(3-Chloro-4-fluorophenyl)-2-(4-((2,4-dioxothiazolidin-5-ylidene)methyl)phenoxy)acetamide (3N). Yield 84.5%; analytical HPLC purity = 98.34%; yellow solid. ^{1}H NMR (400 MHz, DMSO-d_6): δ 12.54 (s, 1H), 10.36 (s, 1H), 7.96−7.94 (m, 2H), 7.76 (s, 1H), 7.60−7.54 (m, 3H), 7.40 (t, 1H, J = 8.8 Hz), 7.16 (d, 2H, J = 8.4 Hz), 4.86 (s, 2H). MS (ESI), m/z: 406.08 [M − H]$^-$.

(*Z*)-*N*-(3,4-Difluorophenyl)-2-(4-((2,4-dioxothiazolidin-5-ylidene)methyl)phenoxy)acetamide (3O). Yield 81.5%; analytical HPLC purity = 99.87%; white solid. ^{1}H NMR (400 MHz, DMSO-d_6): δ 12.53 (s, 1H), 10.37 (s, 1H), 7.82−7.77 (m, 1H), 7.75 (s, 1H), 7.58 (d, 2H, J = 8.8 Hz), 7.45−7.38 (m, 2H), 7.15 (d, 2H, J = 8.4 Hz), 4.81 (s, 2H). MS (ESI), m/z: 389.20 [M − H]$^-$.

(*Z*)-2-(4-((2,4-Dioxothiazolidin-5-ylidene)methyl)phenoxy)-*N*-methyl-*N*-phenylacetamide (3P). Yield 79.6%; analytical HPLC purity = 99.91%; yellow solid. ^{1}H NMR (400 MHz, DMSO-d_6): δ 12.52 (s, 1H), 7.73 (s, 1H), 7.52−7.50 (m, 6H), 7.41 (s, 1H), 6.93 (s, 2H), 4.53 (s, 2H), 3.20 (s, 3H). MS (ESI), m/z: 367.20 [M − H]$^-$.

(*Z*)-*N*-Cyclohexyl-2-(4-((2,4-dioxothiazolidin-5-ylidene)methyl)phenoxy)acetamide (3Q). Yield 78.3%; analytical HPLC purity = 98.61%; light-yellow solid. ^{1}H NMR (400 MHz, DMSO-d_6): δ 12.53 (s, 1H), 7.95 (d, 1H, J = 8.0 Hz), 7.75 (s, 1H), 7.56 (d, 2H, J = 8.8 Hz), 7.09 (d, 2H, J = 8.8 Hz), 4.54 (s, 2H), 3.61 (t,1H, J = 3.6 Hz), 1.74 − 1.64 (m, 4H), 1.58−1.55 (m, 1H), 1.31−1.19 (m, 4H), 1.15−1.06 (m, 1H). MS (ESI), m/z: 359.07 [M − H]$^-$.

(*Z*)-*N*-Benzyl-2-(4-((2,4-dioxothiazolidin-5-ylidene)methyl)-phenoxy)acetamide (3R). Yield 84.3%; analytical HPLC purity = 98.58%; yellow solid. ^{1}H NMR (400 MHz, DMSO-d_6): δ 12.54 (s, 1H), 8.70 (t, 1H, J = 6.0 Hz), 7.76 (s, 1H), 7.57 (d, 2H, J = 8.8 Hz), 7.32−7.31 (m, 2H), 7.25−7.21 (m, 3H), 7.12 (d, 2H, J = 8.8 Hz), 4.65 (s, 2H), 4.34 (d, 2H, J = 6.0 Hz). MS (ESI), m/z: 367.15 [M − H]$^-$.

(*Z*)-2-(4-((2,4-Dioxothiazolidin-5-ylidene)methyl)phenoxy)-*N*-(pyridin-2-yl)acetamide (3S). Yield 65.8%; analytical HPLC purity = 98.05%; light-yellow solid. ^{1}H NMR (400 MHz, DMSO-d_6): δ 12.53 (s, 1H), 10.62 (s, 1H), 8.35 (d, 1H, J = 8.0 Hz), 8.04 (d, 1H, J = 8.0 Hz), 7.83−7.75 (m, 2H), 7.75 (s, 1H), 7.58 (d, 2H, J = 8.8 Hz), 7.16−7.12 (m, 3H), 4.89 (s, 2H). MS (ESI), m/z: 354.03 [M − H]$^-$.

(*Z*)-2-(4-((2,4-Dioxothiazolidin-5-ylidene)methyl)phenoxy)-*N*-(5-methylpyridin-2-yl)acetamide(3T). Yield 74.1%; analytical HPLC purity = 98.29%; light-yellow solid. ^{1}H NMR (400 MHz, DMSO-d_6): δ 12.54 (s, 1H), 10.53 (s, 1H), 8.18 (q, 1H, J = 3.2 Hz), 7.95 (d, 1H, J = 7.6 Hz), 7.76 (s, 1H), 7.64−7.61 (m, 1H), 7.58 (d, 2H, J = 8.8 Hz), 7.13 (d, 2H, J = 9.2 Hz), 4.88 (s, 2H), 2.26 (s, 3H). MS (ESI), m/z: 368.16 [M − H]$^-$.

(*Z*)-2-(4-((2,4-Dioxothiazolidin-5-ylidene)methyl)phenoxy)-*N*-(naphthalen-1-yl)acetamide (3U). Yield 68.3%; analytical HPLC purity = 98.77%; light-yellow solid. ^{1}H NMR (400 MHz, DMSO-d_6): δ 12.54 (s, 1H), 10.21 (s, 1H), 8.00−7.94 (m, 2H), 7.81 (d, 2H, J = 8.0 Hz), 7.78 (s, 1H), 7.66−7.61 (m, 3H), 7.55−7.61 (m, 3H), 7.23 (d, 2H, J = 8.0 Hz), 4.98 (s, 2H). MS (ESI), m/z: 403.05 [M − H]$^-$.

(*Z*)-2-(4-((2,4-Dioxothiazolidin-5-ylidene)methyl)phenoxy)-*N*-(naphthalen-2-yl)acetamide (3V). Yield 70.0%; analytical HPLC purity = 99.22%; white solid. ^{1}H NMR (400 MHz, DMSO-d_6): δ 12.54 (s, 1H), 10.38 (s, 1H), 8.32 (s, 1H), 7.90−7.82 (m, 3H), 7.77 (s, 1H), 7.68−7.65 (m, 1H), 7.60 (d, 2H, J = 8.8 Hz), 7.48 (t, 1H, J = 7.2 Hz), 7.42 (t, 1H, J = 7.2 Hz), 7.20 (d, 2H, J = 8.8 Hz), 4.88 (s, 2H). MS (ESI), m/z: 403.10 [M − H]$^-$.

■ ASSOCIATED CONTENT

Supporting Information. ^{1}H NMR and MS analysis of **1A**−**V**, **2A**−**V**, and **3I**; the detailed HPLC analysis of **3A**−**V**; docking results of all molecules with murine iNOS. This material is available free of charge via the Internet at http://pubs.acs.org.

■ AUTHOR INFORMATION

Corresponding Author

*For M.-L.X.: phone, +86-28-85164103; E-mail, tmkxiang@gmail.com. For L.-J.C.: phone, +86-28-85164063; fax, +86-28-85164060; E-mail, lijuan17@hotmail.com.

Author Contributions

§These authors contributed equally and should be considered co-first authors.

■ ACKNOWLEDGMENT

We are grateful to the National Key Programs of China during the 11th Five-Year Plan period (2009ZX09102-045 and 2009ZX09501-015).

■ ABBREVIATIONS USED

RA, rheumatoid arthritis; NO, nitric oxide; PEG_2, prostaglandin E_2; iNOS, inducible nitric oxide synthase; eNOS, endothelial nitric oxide synthase; nNOS, neuronal nitric oxide synthase; COX, cyclooxygenase; IL-1β, interleukin-1β; TNF-α, tumor necrosis factor-α; NADPH, nicotinamide adenine dinucleotide phosphate; LPS, lipopolysaccharide; TZDs, thiazolidinediones; PPAR-γ, peroxisome proliferator-activated receptor-γ; IR, inhibitory rate; IC_{50}, half maximal inhibitory concentration; AIA, adjuvant-induced arthritis; NMR, nuclear magnetic resonance; MS, mass spectrometry; HPLC, high performance liquid chromatography; DMSO, dimethylsulfoxide; H&E, hematoxylin and eosin

■ REFERENCES

(1) Ruslan, M. Inflammation 2010: New adventures of an old flame. *Cell* **2010**, *140*, 771–776.

(2) Ruslan, M. Origin and physiological roles of inflammation. *Nature* **2008**, *454*, 428–435.

(3) Carl, N. Points of control in inflammation. *Nature* **2002**, *420*, 846–852.

(4) MacMicking, J.; Xie, Q. W.; Nathan, C. Nitric oxide and macrophage function. *Annu. Rev. Immunol.* **1997**, *15*, 323–350.

(5) Giuseppe, C.; Eleonora, D.; Wallace, J. L. Nitric oxide and inflammation. *Inflammation Allergy: Drug Targets.* **2006**, *5*, 115–119.

(6) Clancy, R. M.; Amin, A. R.; Abramson, S. B. The role of nitric oxide in inflammation and immunity. *Arthritis Rheum.* **1998**, *41*, 1111–1151.

(7) Hobbs, A. J.; Higgs, A.; Moncada, S. Inhibition of nitric oxide synthase as a potential therapeutic target. *Annu. Rev. Pharmacol. Toxicol.* **1999**, *39*, 191–220.

(8) Alderton, W. K.; Cooper, C. E.; Knowles, R. G. Nitric oxide synthases: structure, function and inhibition. *Biochem. J.* **2001**, *357*, 593–615.

(9) György, N.; Joanna, M. C.; Edit, I. B.; Claire, L. G.; Andrew, P. C. Nitric oxide, chronic inflammation and autoimmunity. *Immunol. Lett.* **2007**, *111*, 1–5.

(10) Daniel, L. S.; Regina, M. B.; Timothy, H. L. A. Cyclooxygenase isozymes: the biology of prostaglandin synthesis and inhibition. *Pharmacol. Rev.* **2004**, *56*, 387–437.

(11) Takuya, K.; Shuh, N. Function of prostanoid receptors: studies on knockout mice. *Prostaglandins Other Lipid Mediators* **2002**, *68*—*69*, 557–573.

(12) Yki-Jarvinen, H. Drug Therapy—Thiazolidinediones. *N. Engl. J. Med.* **2004**, *351*, 1106–1118.

(13) Collin, M.; Thiemermann, C. The PPAR-γ ligand 15-deoxy$^{\Delta 12,14}$ prostaglandin J_2 ver injury in endotoxic shock. *Eur. J. Pharmacol.* **2003**, *29*, 257–258.

(14) Yumei, Y.; Yu, L.; Saraswathy, M.; Brian, C. T.; Yochai, B. Pioglitazone protects the myocardium against ischemia-reperfusion injury in eNOS and iNOS knockout mice. *Am. J. Physiol.: Heart. Circ. Physiol.* **2008**, *295*, 2436–2446.

(15) Crosby, M. B.; Svenson, J. L.; Zhang, J.; Nicol, C. J.; Gonzalez, F. J.; Gilkeson, G. S. PPAR {gamma} is not necessary for synthetic PPAR {gamma} agonist inhibition of iNOS and nitric oxide. *J. Pharmacol. Exp. Ther.* **2005**, *12*, 69–76.

(16) Ricote, M.; Li, A. C.; Willson, T. M.; Kelly, C. J.; Glass, C. K. The peroxisome proliferator-activated receptor-γ is a negative regulator of macrophage activation. *Nature* **1998**, *391*, 79–82.

(17) Michelle, B. C.; John, S.; Gary, S. G.; Tamara, K. N. A novel PPAR response element in the murine iNOS promoter. *Mol. Immunol.* **2005**, *42*, 1303–1310.

(18) Camps, M.; Ruckle, T.; Ji, H.; Ardissone, V.; Rintelen, F.; Shaw, J.; Ferrandi, C.; Chabert, C.; Gillieron, C.; Francon, B.; Martin, T.; Gretener, D.; Perrin, D.; Leroy, D.; Vitte, P. A.; Hirsch, E.; Wymann, M. P.; Cirillo, R.; Schwarz, M. K.; Rommel, C. Blockade of PI3K suppresses joint inflammation and damage in mouse models of rheumatoid arthritis. *Nature Med.* **2005**, *11*, 936–941.

(19) Bruno, G.; Costantino, L.; Curinga, C.; Maccari, R.; Monforte, F.; Nicolo, F.; Ottana, R.; Vigorita, M. G. Synthesis and aldose reductase inhibitory activity of 5-arylidene- 2,4-thiazolidinediones. *Bioorg. Med. Chem.* **2002**, *10*, 1077–1084.

(20) Xu, Z.; Knaak, C.; Ma, J.; Beharry, Z. M.; Mcinnes, C.; Wang, W.; Kraft, A. S.; Smith, C. D. Synthesis and Evaluation of Novel Inhibitors of Pim-1 and Pim-2 Protein Kinases. *J. Med. Chem.* **2009**, *52*, 74–86.

(21) Momose, Y.; Meguro, K.; Ikeda, H.; Hatanaka, C.; Oi, S.; Sohda, T. Studies on Antidiabetic Agents. X. Synthesis and Biological Activities of Pioglitazone and Related Compounds. *Chem. Pharm. Bull.* **1991**, *39*, 1440–1445.

(22) Tihomir, T.; Nace, Z.; Manica, M. P.; Danijel, K.; Lucija, P. M. Synthesis and antibacterial activity of 5-ylidenethiazolidin-4-ones and 5-benzylidene-4,6-pyrimidine-diones. *Eur. J. Med. Chem.* **2010**, *45*, 1667–1672.

(23) Nace, Z.; Jure, K.; Danijel, K. A Convenient Synthesis of 4-Benzyl-2-(2-(4-oxo-2-thioxothiazolidin-5-ylidene)ethyl)-2*H*-1, 4-benzoxazin-3(4*H*)-ones and 5-(2-(4-Benzyl-3-oxo-3,4-dihydro-2*H*-1,4-benzoxazin-2-yl)ethylidene)thiazolidine-2,4-diones. *Acta. Chim. Slov.* **2009**, *56*, 635–642.

(24) Toshimasa, I.; Yasuko, I.; Masatoshi, I.; Yoko, U.; Chiaki, T. Structural elucidation of epalrestat (ONO-2235), a potent aldose reductase inhibitor, and isomerization of its double bonds. *Tetrahedron Lett.* **1989**, *30*, 959–962.

(25) Zidar, N.; Tomasić, T.; Sink, R.; Rupnik, V.; Kovac, A.; Turk, S.; Patin, D.; Blanot, D.; Contreras, M. C.; Dessen, A.; Müller, P. M.; Zega, A.; Gobec, S.; Peterlin, M. L; Kikelj, D. Discovery of novel 5-benzylidenerhodanine and 5-benzylidenethiazolidine-2,4-dione inhibitors of MurD ligase. *J. Med. Chem.* **2010**, *53*, 6584–6594.

(26) Hart, F.; Boardman, P. Indomethacin: q new nonsteroid anti-inflammatory agent. *Br. Med. J.* **1963**, *5363*, 965–70.

(27) Humphrey, W.; Dalke, A.; Schulten, K. VMD—Visual Molecular Dynamics. *J. Mol. Graphics* **1996**, *14*, 33–38.

(28) Knowles, R. G.; Moncada, S. Nitric oxide synthase in mammals. *Biochem. J.* **1994**, *298*, 249–258.

(29) Clive, D. M.; Stoff, J. S. Renal syndromes associated with nonsteroidal anti-inflammatory drugs. *New Engl. J. Med.* **1984**, *310*, 563–572.

(30) Corriveau, C. C.; Danner, R. L. Endotoxin as a therapeutic target in septic shock. *Infect. Agents. Dis.* **1993**, *2*, 35–43.

(31) Kubes, P.; McCafferty, D. M. Nitric oxide and intestinal inflammation. *Am. J. Med.* **2000**, *109*, 150–158.